

## RESEARCH ARTICLE

# Leiomodins 3 and tropomodulin 4 have overlapping functions during skeletal myofibrillogenesis

Chinedu U. Nworu, Robert Kraft, Daniel C. Schnurr, Carol C. Gregorio\* and Paul A. Krieg

## ABSTRACT

Precise regulation of thin filament length is essential for optimal force generation during muscle contraction. The thin filament capping protein tropomodulin (Tmod) contributes to thin filament length uniformity by regulating elongation and depolymerization at thin filament ends. The leiomodins (Lmod1–3) are structurally related to Tmod1–4 and also localize to actin filament pointed ends, but *in vitro* biochemical studies indicate that Lmods act instead as robust nucleators. Here, we examined the roles of Tmod4 and Lmod3 during *Xenopus* skeletal myofibrillogenesis. Loss of Tmod4 or Lmod3 resulted in severe disruption of sarcomere assembly and impaired embryonic movement. Remarkably, when Tmod4-deficient embryos were supplemented with additional Lmod3, and Lmod3-deficient embryos were supplemented with additional Tmod4, sarcomere assembly was rescued and embryonic locomotion improved. These results demonstrate for the first time that appropriate levels of both Tmod4 and Lmod3 are required for embryonic myofibrillogenesis and, unexpectedly, both proteins can function redundantly during *in vivo* skeletal muscle thin filament assembly. Furthermore, these studies demonstrate the value of *Xenopus* for the analysis of contractile protein function during *de novo* myofibril assembly.

**KEY WORDS:** Actin thin filament, Leiomodins, Sarcomere, Skeletal muscle, Tropomodulin

## INTRODUCTION

Precise regulation of actin thin filament length in striated muscle is essential for efficient contractile force generation and cellular function (Granzier et al., 1991; Gregorio et al., 1995; Witt et al., 2006; Bang et al., 2006; Ottenheim et al., 2009; Gokhin et al., 2009). Understanding the mechanisms by which actin thin filaments assemble and maintain precisely uniform lengths while undergoing dynamic turnover and generating contractile force remains an area of active investigation. One of the most intensively studied regulators of thin filament length is the actin filament capping protein tropomodulin1 (Tmod1). In vertebrates, there are four related Tmod family proteins with distinct expression patterns. Tmod1 is expressed prominently in postmitotic, terminally differentiated cells, including striated muscle, erythrocytes, lens fiber cells and neurons (for a recent review, see Yamashiro et al., 2012). In striated muscle, in

cooperation with tropomyosin, Tmod1 binds to and limits the exchange of actin monomers at the pointed end of the actin thin filaments (Weber et al., 1994). The localization and capping functions of Tmod1 appear to be dependent on two actin-binding and two tropomyosin-binding domains, given that mutations in any of these regions affect these functions (Fowler et al., 2003; Kostyukova et al., 2005; Kostyukova et al., 2006; Greenfield et al., 2005; Kong and Kedes, 2006; Tsukada et al., 2011). Overexpression of Tmod1 in primary myocyte cultures results in a shortening of actin filaments (Sussman et al., 1999; Littlefield et al., 2001), whereas depletion of Tmod1 leads to abnormally long thin filaments (Gregorio et al., 1995; Sussman et al., 1998; Mudry et al., 2003). Mouse embryos null for Tmod1 die at embryonic day (E)9.5–10.5 owing to cardiac defects (Fritz-Six et al., 2003; Chu et al., 2003; McKeown et al., 2008). Although Tmod1 is expressed in skeletal muscle, the assembly and maintenance of skeletal muscle myofibrils appears to be normal in Tmod1-null embryos (Gokhin et al., 2010).

Tmod4 is the predominant Tmod isoform in mammalian skeletal muscle, where it is believed to play a role equivalent to that of Tmod1 in cardiac muscle (Almenar-Queralt et al., 1999a; Almenar-Queralt et al., 1999b; Gokhin et al., 2010). The relative ratios of Tmod1 and Tmod4 in mammalian skeletal muscle have not been measured directly but appear to be correlated with muscle twitch speed, with Tmod4 predominating in fast-twitch skeletal muscle (Almenar-Queralt et al., 1999b). Tmod4 is also reported to associate with either the sarcomeric reticulum or T-tubule-associated membrane compartment at the Z-line (Gokhin and Fowler, 2011).

Tmod2 is expressed primarily in adult neuronal tissue (Watakabe et al., 1996; Conley et al., 2001), whereas Tmod3 is considered to be ubiquitous. In murine skeletal muscle, Tmod3 is thought to stabilize cytoplasmic  $\gamma$ -actin (nonmuscle) filaments in the sarcoplasmic reticulum (Gokhin and Fowler, 2011). In addition, in adult Tmod1-null muscles, Tmod3 translocates from extrasarcomeric sites to cap thin filament pointed ends together with Tmod4, thus maintaining correct thin filament length and sarcomere organization, structurally compensating for the absence of Tmod1 as skeletal muscle matures (Gokhin and Fowler, 2011; Gokhin et al., 2010).

Rather less is known about the expression and function of the leiomodins (Lmod) family of proteins, Lmod1, Lmod2 and Lmod3. These three vertebrate proteins exhibit distinct adult tissue distributions, with Lmod1 reported to be smooth-muscle-specific, whereas Lmod2 and Lmod3 are present in both cardiac and skeletal muscle (Conley et al., 2001; Nanda and Miano, 2012). Antibody and overexpression studies indicate that Lmod2 is present at the M-line region of the sarcomere in cardiac myofibrils (Chereau et al., 2008; Tsukada et al., 2010; Skwarek-Maruszewska et al., 2010). During chick embryo development,

Department of Cellular and Molecular Medicine, Sarver Molecular Cardiovascular Research Program, University of Arizona, 1656 E. Mabel St, Tucson, AZ 85724, USA.

\*Author for correspondence (gregorio@email.arizona.edu)

transcript studies revealed Lmod2 to be expressed in the heart shortly after the start of cardiac contractions, which is significantly later than the expression of Tmod1, the major Tmod isoform expressed in heart (Tsukada et al., 2010). Although the Lmods share some structural similarities to the Tmods, there are also substantial differences. Lmods lack the second tropomyosin-binding domain present in Tmods but possess an additional (third) actin-binding domain within the extended C-terminal region (Fig. 1A; Conley et al., 2001). In contrast to Tmods, biochemical studies indicate that Lmods function to robustly nucleate actin filament formation *in vitro* (Chereau et al., 2008). Furthermore, whereas Tmods have the ability to limit the polymerization of (cap) actin filaments in biochemical assays, Lmods fail to exhibit this property (Weber et al., 1994; Tsukada et al., 2010). When the C-terminal extension of Lmod2 is deleted, however, the truncated Lmod can function as a capping protein *in vitro*, suggesting that the C-terminal extension modulates the biochemical properties of the Lmods (Tsukada et al., 2010). Finally, it was discovered that overexpression of Lmod2 in cultured rat cardiomyocytes results in elongation of the actin

filament and displacement of Tmod1 at the end of the filament (Tsukada et al., 2010). Based on these observations, it appears that Lmod2 functions as an antagonist of Tmod1, and that a balance between Tmod and Lmod protein activities is required for correct thin filament length regulation.

The results presented here show that Tmod4 and Lmod3 are the predominant isoforms expressed in developing skeletal muscle in the *Xenopus* embryo and that expression of both transcripts precedes myofibrillogenesis. Reducing the protein levels of either Tmod4 or Lmod3 severely compromises sarcomere assembly. Unexpectedly, we determined that Lmod3 and Tmod4 can structurally and physiologically compensate for each other during myofibrillogenesis. Taken together, our results show that sufficient levels of both Tmod4 and Lmod3 are required for normal skeletal muscle development in *Xenopus*, and that the two proteins share largely redundant functions during sarcomere assembly. Moreover, our studies demonstrate that the *Xenopus* embryo is a powerful system to study the functional properties of specific contractile components during *de novo* myofibril assembly.

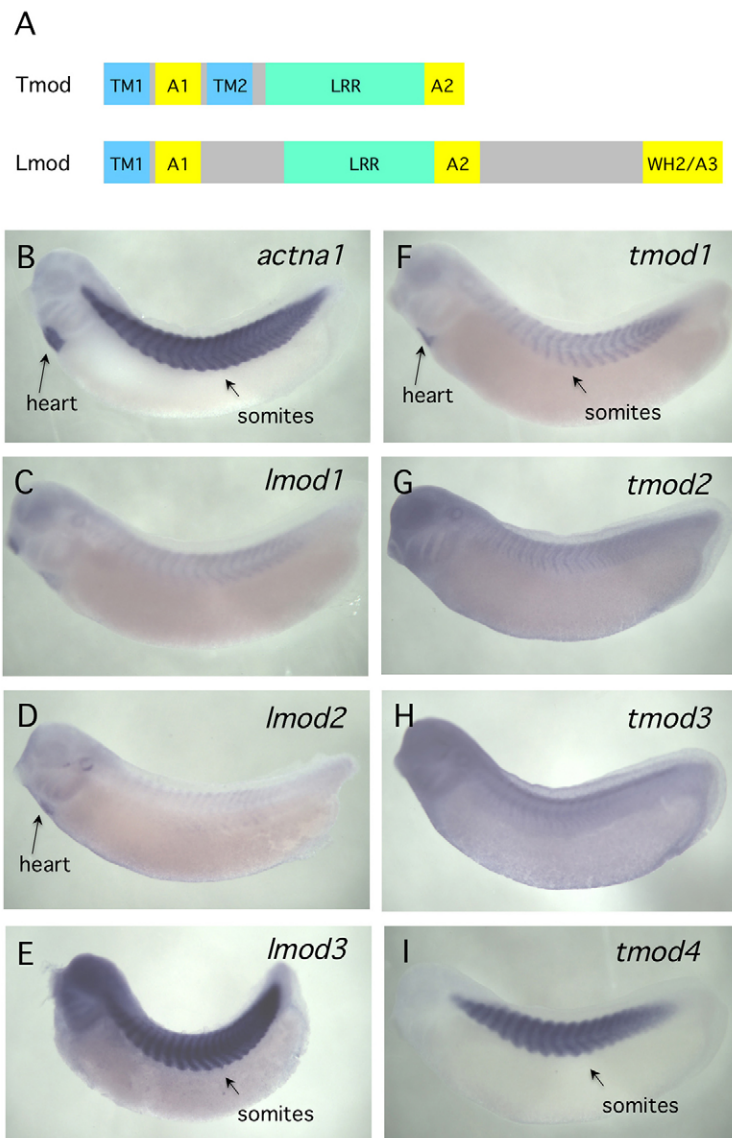


**Fig. 1. Structure and developmental expression of the leiomodins (Lmod) and tropomodulins (Tmod) gene families.**

(A) leiomodins (Lmod1–3) and tropomodulins (Tmod1–4) proteins are structurally related, yet possess unique domains. Lmods and Tmods share actin-binding (A1, A2), tropomyosin-binding (TM1) and leucine-rich-repeat (LRR) domains. A second tropomyosin-binding domain (TM2) is unique to the Tmods. Lmod proteins have a C-terminal extension that contains a third actin binding/WH2 domain (WH2/A3). (B–I) Lmod (C–E) and Tmod (F–I) family gene expression was analyzed during *Xenopus* embryonic development using *in situ* hybridization. All embryos are positioned with heads to the left. Expression patterns are shown at the early tailbud stage (st30), during the early stages of myofibrillogenesis. Earlier expression during the neurula stage (st15) is presented in supplementary material Fig. S1. Expression of the definitive striated muscle marker cardiac actin, *actna1* (B), was used to indicate cardiac and skeletal muscle tissue in the embryo. Arrows indicate developing skeletal muscle and heart tissues. Only *lmod3* (E) and *tmod4* (I) are expressed at high levels in developing skeletal muscle.

## RESULTS

**Tmod4 and Lmod3 transcripts are expressed during all stages of myofibril assembly**

Using information from DNA sequence databases, we have identified all genes of the Tmod (Tmod1–4) and Lmod (Lmod1–3) families of *Xenopus laevis*. Both primary sequence conservation and syntenic organization allow unambiguous identification of the *Xenopus* Tmod and Lmod genes with the orthologous mammalian genes. Previous work by others has recognized the significant structural similarity between the Tmod and Lmod families of proteins (Conley et al., 2001; Fig. 1A), including two conserved actin-binding domains (A1 and A2). However, there are also significant differences between the Lmod and Tmod proteins, such as the absence of the second tropomyosin-binding site (TM2) from Lmod and the presence of an additional actin-binding domain (A3) in the C-terminal extension found only in Lmod proteins (Conley et al., 2001).

By using *in situ* hybridization, we determined the tissue-specific expression patterns of the *tmod* and *lmod* gene families in the *Xenopus* embryos (Fig. 1C–I; supplementary material Fig. S1). These were compared to the pattern of cardiac actin, *actn1* (Fig. 1B), which is a highly specific marker of striated muscle (Mohun et al., 1984). Examination of *lmod1–3* gene expression patterns (Fig. 1C–E) showed that *lmod1* was expressed at potentially trace amounts in the heart and weakly in developing somites (skeletal muscle), whereas *lmod2* was expressed weakly in the early heart. In contrast, *lmod3* was expressed very strongly in skeletal muscle but was absent from the heart (Fig. 1E). For the *tmod* gene family, expression of *tmod1* was visible in the early

heart and weakly visible in skeletal muscle, whereas the staining pattern for *tmod2* and *tmod3* was generally diffuse and consistent with non-specific background staining. Transcripts for *tmod4* were highly abundant in skeletal muscle but not in the developing cardiac muscle (Fig. 1I). Importantly for the subsequent experiments in this report, *tmod4* and *lmod3* are expressed at high levels in developing skeletal muscle tissues, whereas the other family members are expressed at low or undetectable levels.

**Tmod4 and Lmod3 localize and assemble in the M-line region during *de novo* myofibrillogenesis**

Our studies are directed towards understanding the roles of Tmod4 and Lmod3 proteins during the initial assembly of the skeletal muscle sarcomere. To better characterize the experimental model, we examined the expression and subcellular localization of Tmod4 and Lmod3 during early skeletal muscle development (Fig. 2). Analysis was performed at three developmental stages, which were centered on the time at which myofibrillogenesis first occurs within *Xenopus* somites. First, we analyzed the localization of Tmod4 (Fig. 2A–L). At the earliest time-point analyzed [stage (st)20], organized sarcomeres were not visible. Phalloidin staining detected nonstriated filamentous actin (i.e. thin filaments of equal or different lengths that are not aligned), and staining for the prominent Z-disc marker  $\alpha$ -actinin detected isolated dot-like puncta. These observations are identical to descriptions of myofibrillogenesis in other well-characterized organisms (for reviews, see Sparrow and Schöck 2009; Ono 2010). Although Tmod4 is expressed at this stage, its localization is not organized (compare Fig. 2C,K). Effectively identical

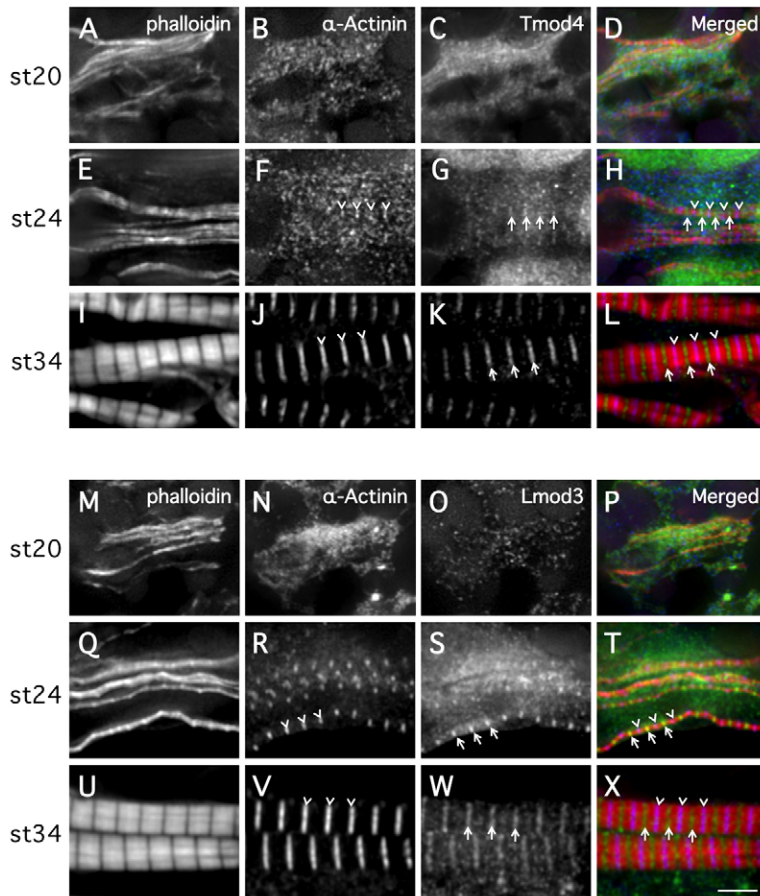


**Fig. 2. Tmod4 and Lmod3 localize to the M-line during *Xenopus* skeletal myofibrillogenesis.** The somite regions of *Xenopus* embryos were sectioned and protein distribution was examined using Texas-Red-conjugated phalloidin and antibodies against  $\alpha$ -actinin, Tmod4 or Lmod3. (A–L) Localization of Tmod4 protein during skeletal muscle myofibrillogenesis. (A–D) At st20, continuous actin filament staining was visible (A), with no periodic localization of  $\alpha$ -actinin (B) or Tmod4 staining (C). (E–H) At st24, diffuse striations were visible in a small number of actin filaments (E). In these striated regions, narrow bands of  $\alpha$ -actinin (F, arrowheads) and Tmod4 staining (G, arrows) were visible. (I–L) At st34, broad sharply striated (i.e. highly organized) actin filaments (I) were observed throughout the skeletal muscle tissue. Sharp regions of  $\alpha$ -actinin (J, arrowheads) and Tmod4 staining (K) were visible at the Z-disc and M-line regions, respectively. (M–X) Localization of Lmod3 protein during skeletal muscle myofibrillogenesis. (M–P) At st20, continuous actin filament staining was visible, but no localization of  $\alpha$ -actinin (N) or Lmod3 (O) was observed. (Q–T) At st24, some regions of developing muscle showed narrow diffusely striated actin filaments (Q). In these regions, narrow bands of  $\alpha$ -actinin (R, arrowheads) and Lmod3 staining (S, arrows) were visible. (U–X) At st34, broad sharply striated actin filaments were visible throughout the developing somites. Staining for  $\alpha$ -actinin (V, arrowheads) and Lmod3 (W, arrows) was detected at the Z-line and M-line regions, respectively. We conclude that both Tmod4 and Lmod3 proteins are present at the M-line region of the sarcomere from the earliest stages of myofibril assembly. Scale bar: 5  $\mu$ m.

observations were made for Lmod3 at the same stage, with Lmod3 staining appearing as randomly distributed aggregates with no clear organization (Fig. 2O). We next examined somite tissue ~5 hours later, at the time of the earliest detectable sarcomere formation in *Xenopus* (st24, Huang and Hockaday, 1988). At this stage, some nascent sarcomeres (often referred to as ‘Z-bodies’ or ‘I-Z-I-like structures’; Rhee et al., 1994; Holtzer et al., 1997) were visible with phalloidin and  $\alpha$ -actinin staining (Fig. 2E). Although most  $\alpha$ -actinin appeared punctate, regularly spaced striations were visible in the same regions that exhibited striated phalloidin staining (Fig. 2F, arrowheads). The regions of myogenic tissue containing organized  $\alpha$ -actinin and F-actin showed the presence of Tmod4 at the M-line region of the nascent sarcomere (Fig. 2G,H, arrows). Once again, the pattern of Lmod3 staining was nearly identical to that observed for Tmod4, with clear narrow striations of Lmod3 staining at nascent M-lines (Fig. 2S,T). At the sarcomere length present in developing *Xenopus* muscle, staining at thin filament pointed ends was observed as a single band, rather than as a doublet representing molecules from both sides of the sarcomere. Finally, we examined sarcomere assembly in the skeletal muscle of tailbud embryos (st32), ~15 hours after the first sarcomeres were detected. In these embryos, highly organized myofibrils were visible throughout the somites (Fig. 2I–L). Both Tmod4 (Fig. 2K,L) and Lmod3 (Fig. 2W,X) were observed at the M-lines of mature sarcomeres. Based on these observations, we conclude that both Tmod4 and Lmod3 proteins are present in *Xenopus* myogenic tissue at the earliest stages of myofibrillogenesis and are localized in close proximity to the M-line as early as sarcomeres are visible.

#### Depletion of Tmod4 prevents sarcomere assembly

Little is known about the role of Tmod4 during sarcomere assembly *in vivo*. To address this issue, we used an antisense morpholino (MO) to specifically reduce Tmod4 expression during early *Xenopus* development. Embryos injected with *tmod4* MO or control MO were allowed to develop until the tailbud stage, when they were prepared for immunofluorescence microscopy or for western blot analysis. Although western blots demonstrated that Tmod4 levels were reduced dramatically (>90%) by the MO treatment (Fig. 3B), the treated embryos showed remarkably normal external appearance (Fig. 3A). Deconvolution microscopy was used to examine the localization of Z-disc, thin filament, thick filament and titin proteins on frozen sections of somite tissue from control (Fig. 3C–F) and Tmod4-knockdown (Fig. 3G–J) embryos. Assays were carried out at st34 because highly ordered sarcomeres are present throughout the trunk region of wild-type embryos by this stage (Fig. 2I–L,U–X). Control embryos exhibited well-organized Z-discs marked by  $\alpha$ -actinin, well-organized thin filaments and Tmod4 staining (Fig. 3C). In contrast, near complete disruption of myofibrils was observed in the somites from Tmod4-knockdown embryos (Fig. 3G). Specifically,  $\alpha$ -actinin was organized as isolated puncta or in irregular striations, whereas phalloidin staining showed no regular pattern. The distribution of titin and myosin was also perturbed (compare Fig. 3L,P,M,Q). To address the possibility that sarcomeres formed normally in knockdown embryos but were subsequently disrupted (i.e. that Tmod4 might be required for myofibril maintenance), timecourse studies were performed. These experiments revealed that sarcomeres never assembled in Tmod4-depleted embryos, even at the earliest stages of development (data not shown).

Although western blots showed very effective reduction of Tmod4 protein levels in MO-treated embryos (Fig. 3B), we considered the possibility that other *tmod* or *lmod* genes might undergo transcriptional upregulation in an effort to compensate for the absence of Tmod4. We used *in situ* hybridization to examine the levels of all *tmod* and *lmod* transcripts in control MO and *tmod4* MO-treated embryos (supplementary material Fig. S2). The assay was performed at the same developmental stage at which sarcomere structure was examined (st34). These studies showed that gene expression for *tmod* and *lmod* genes was not detectably altered in response to *tmod4* MO treatment. Therefore, the results observed in subsequent experiments should be independent of compensatory expression of endogenous Lmod and Tmod proteins.

To confirm that the lack of sarcomere structure was due to loss of Tmod4 and was not a non-specific effect of MO treatment, we carried out rescue experiments. As a preliminary control, we introduced mRNA encoding GFP–Tmod4 into untreated embryos and demonstrated that it localized to the appropriate position at the M-line, indistinguishable from the location of endogenous Tmod4 (Fig. 3T; supplementary material Fig. S3A–D). No alteration in dimensions or structure of the myofibrils was observed at the doses of GFP–Tmod4 used for the rescue studies (Table 1; supplementary material Fig. S3A–D). To directly test whether the addition of Tmod4 could rescue myofibril structure in *tmod4* MO-treated embryos, we introduced mRNA encoding GFP–Tmod4 into the embryo together with the *tmod4* MO (supplementary material Fig. 3S–V). Examination of the resulting somites showed that addition of GFP–Tmod4 effectively restored overall myofibril assembly as assessed by observation of  $\alpha$ -actinin, F-actin, titin and myosin organization (Fig. 3S–Z). Additionally, quantification showed that thin filament lengths (TFLs) and sarcomere lengths in Tmod4-rescued embryos were comparable to those of unmanipulated embryos (Table 1). In view of the success of the rescue studies, we conclude that specific ablation of Tmod4 is responsible for the loss of sarcomere assembly. From multiple experiments, we determined that addition of GFP–Tmod4 to the MO-treated embryos produced a significant increase in organized sarcomere structure, as assessed by the presence of M-line gaps in phalloidin staining, compared with the Tmod4-depleted embryos (Fig. 3Aa, 62.5% versus 5.9%). Taken together, these studies demonstrate that Tmod4 is essential for *de novo* myofibril assembly in skeletal muscle.

#### Depletion of Lmod3 prevents sarcomere assembly

We carried out a similar series of experiments examining the role of Lmod3 during embryonic skeletal muscle development. First, we demonstrated that the addition of a sequence-specific *lmod3* MO effectively depleted Lmod3 expression (>90%) in embryonic muscle while having little detectable effect on overall embryonic development (Fig. 4A,B). Staining of somites from tailbud-stage embryos depleted of Lmod3 revealed a complete absence of organized sarcomeres compared with controls (Fig. 4C–R). As previously observed for Tmod4 depletion (Fig. 3H,I),  $\alpha$ -actinin localization was punctate and phalloidin staining was nonstriated (i.e. no clear repeating organization of actin filaments) (Fig. 4H,I). The organization of titin and myosin was also disordered (Fig. 4P,Q). Although, in most areas, phalloidin staining was nonstriated, sarcomeres with organized thin filaments were observed in some regions (~24%). For rescue studies, we first

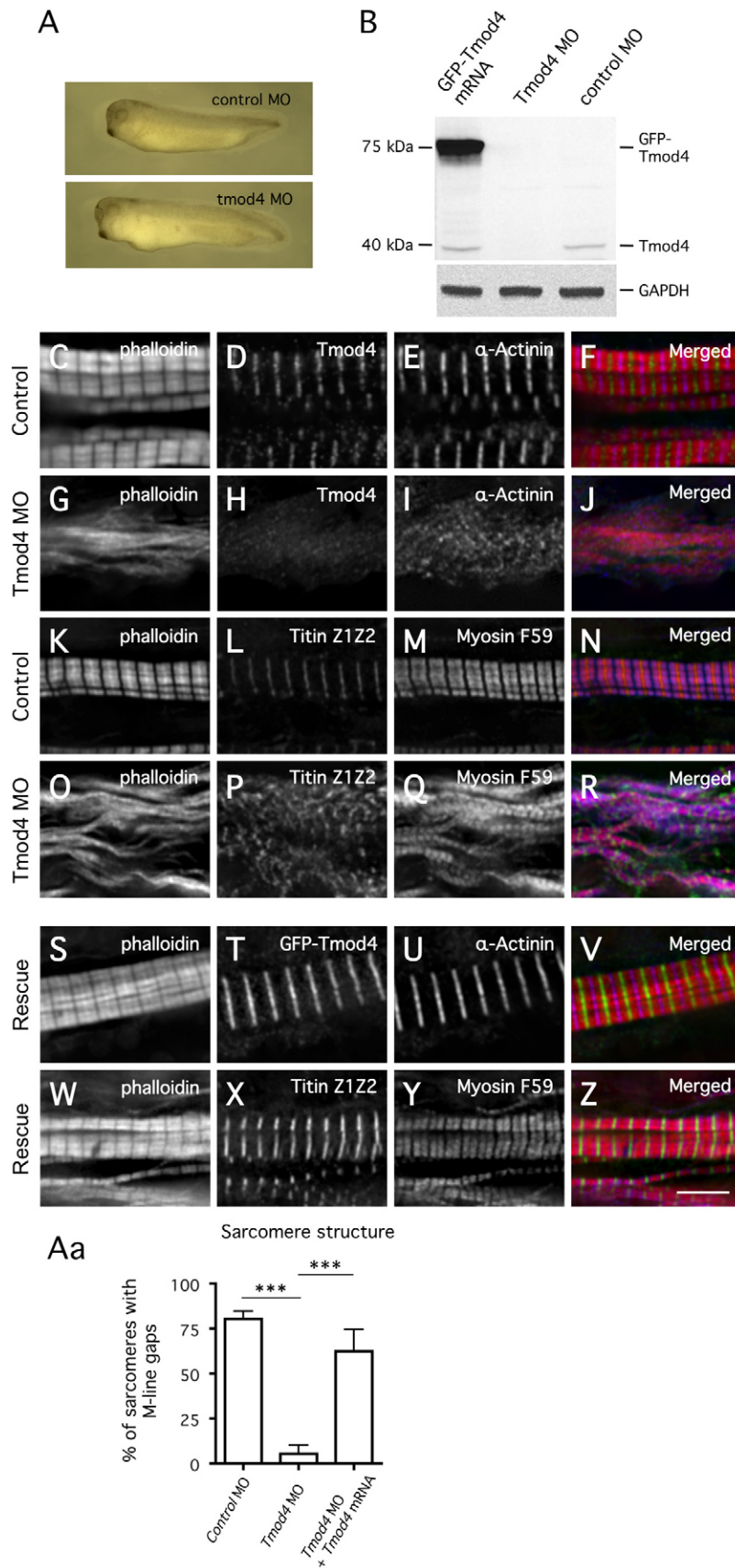


**Fig. 3. Tmod4 is essential for skeletal muscle myofibril assembly.** (A) Embryos treated with control MO (upper panel) and *tmod4* MO (lower panel) develop normally. (B) Protein blots demonstrate that the anti-Tmod antibody specifically recognizes *Xenopus* Tmod4 protein (lane labeled GFP-Tmod4) and that the *tmod4* MO effectively blocked translation of Tmod4 protein. (C–R) Loss of Tmod4 protein resulted in disruption of sarcomere assembly. (G–J) Sections through developing muscle tissue of embryos depleted of Tmod4 protein show severely disrupted sarcomeres compared with control embryos at the same developmental stage (C–F). (O–R) Localization of other sarcomeric components, including the N-terminal region of titin (P) and myosin heavy chain (Q) was also severely disorganized compared with that of controls (K–N). (S–Aa) The specificity of the Tmod4 knockdown was demonstrated by rescue experiments. In these studies, *tmod4* MO was co-injected into the *Xenopus* embryo with mRNA encoding GFP-Tmod4. Organization of both thin filament (S–V) and other sarcomeric proteins (X, Y) was comparable to that of unmanipulated controls (C–F). All fluorescent images (C–Z) are presented at the same scale. Scale bar: 5 μm. Quantification of experimental results (Aa) showed that depletion of Tmod4 protein in st34 embryos resulted in a dramatic reduction in the percentage of correctly structured sarcomeres (~5.4% of fibers showing M-line gaps following phalloidin staining compared to 62.5% in controls). Addition of mRNA encoding GFP-Tmod4, together with the MO, resulted in rescue of sarcomere structure. Data show the mean ± s.e.m.; \*\*\**P* < 0.001 ( $\chi^2$  analysis).

**Table 1. Thin filament and sarcomere length analysis**

Experiment	TFL		SL		<i>n</i>
	Mean±s.d. (μm)	Min–max (μm)	Mean±s.d. (μm)	Min–max (μm)	
Control	0.85±0.01	0.80–0.88	2.04±0.05	1.87–2.13	31
GFP–Tmod4	0.83±0.03	0.77–0.91	2.07±0.08	1.84–2.21	62
Myc–Lmod3	0.85±0.03	0.75–0.88	2.05±0.06	1.94–2.16	23
Myc–Lmod3+ <i>lmod3</i> MO	0.83±0.04	0.72–0.89	2.01±0.09	1.85–2.20	26
GFP–Tmod4+ <i>tmod4</i> MO	0.84±0.05	0.74–0.94	2.08±0.13	1.83–2.47	37
GFP–Tmod4+ <i>lmod3</i> MO	0.74±0.04***	0.65–0.86	1.99±0.08*	1.77–2.24	44
Myc–Lmod3 rescue+ <i>tmod4</i> MO	0.86±0.04	0.73–0.96	2.05±0.07	1.87–2.19	56

Thin filament and sarcomere dimensions were equivalent to controls for all treatments except for the GFP–Tmod4 rescue of Lmod3 MO group. TFL, thin filament length; SL, sarcomere length. A Student's *t*-test was used for statistical analysis (\**P*<0.05; \*\*\**P*<0.001).

demonstrated that expression of Myc–Lmod3 alone did not alter myofibril dimensions or structure (supplementary material Fig. S3E–H; Table 1). Second, we showed that disruption of myofibril assembly and actin thin filament (sarcomere) organization caused by *lmod3* MO was efficiently rescued by expression of Myc–Lmod3 (Fig. 4S–Z). The success of the rescue demonstrates that absence of sarcomere structure was due specifically to Lmod3 depletion. Data from multiple experiments showed that addition of Myc–Lmod3 to MO-treated embryos resulted in a significant increase in organized sarcomere structure compared with that of embryos treated with *lmod3* MO alone (Fig. 4I; 70.2% versus 23.6%). Quantification of thin filament lengths revealed that Lmod3-rescued embryos exhibited TFLs and sarcomere lengths that were comparable to those of control embryos (Table 1). These results demonstrate that Lmod3 plays an essential role during the initial stages of myofibril assembly in embryonic skeletal muscle.

#### Tmod4 and Lmod3 exhibit functional equivalence during sarcomere assembly

The Tmod and Lmod protein families share several structural domains (Fig. 1A) and phylogenetic analysis places Tmod and Lmod within a single larger protein family (Conley et al., 2001; and for a review, see Yamashiro et al., 2012). Furthermore, immunofluorescent staining suggests that the Lmod3 and Tmod4 proteins are located at similar or identical positions within the sarcomere, at or near the pointed end of the thin filament (Fig. 2K,W). However, all *in vitro* and cell culture experiments to date suggest that the Lmod and Tmod family members are biochemically and cell biologically distinct (see Introduction). To further explore this issue, we sought to determine whether Tmod4 and Lmod3 proteins might share functional properties during myofibril assembly in embryonic muscle. To test this idea, we attempted to rescue sarcomere formation in Tmod4-depleted muscle, by expression of Myc–Lmod3. Western blot analysis showed that the level of endogenous Lmod3 protein was not altered by *tmod4* MO treatment (data not shown), so the result of adding Myc–Lmod3 was to raise the total amount of Lmod3 protein present during sarcomere formation. When skeletal muscle was examined in Tmod4-depleted embryos supplemented with additional Myc–Lmod3, we observed a striking rescue of sarcomere structure. Although Tmod4-depleted embryos showed little thin filament structure when stained with phalloidin (Fig. 5A), embryos supplemented with Myc–Lmod3 showed a regular striated (i.e. organized) staining pattern with distinct M-line gaps (Fig. 5E). As expected, following Tmod4 depletion, endogenous Tmod4 protein was

not detectable in the M-line region (Fig. 5G), but Myc–Lmod3 protein was observed at this location (Fig. 5F). Assembly of other sarcomere proteins including myosin was also restored following addition of Myc–Lmod3 (Fig. 5I–L). Results from analysis of four experiments are summarized in Fig. 5Y. Based on an overall analysis of sarcomere structure visualized by phalloidin staining, addition of Myc–Lmod3 results in an increase in actin thin filament organization from 4% to 27%, compared with that of samples treated with *tmod4* MO alone. Measurements showed that sarcomere and actin filament lengths in Myc–Lmod3-rescued embryos were not statistically different from those of controls (Table 1). These results indicate that Lmod3 is sufficient to facilitate myofibril assembly in embryonic skeletal muscle, in the near absence of Tmod4.

We next determined whether it was possible to rescue Lmod3 depletion (Fig. 5M–P) by addition of GFP–Tmod4 (Fig. 5Q–X). Similar to the Lmod3 rescue of Tmod4 knockdown described above, the addition of GFP–Tmod4 was sufficient to rescue sarcomere structure in Lmod3-depleted skeletal muscle. Furthermore, triple staining revealed the presence of GFP–Tmod4, but not endogenous Lmod3, at the region of the M-line when organized thin filament structure was evident (Fig. 5R,S). Analysis of multiple experimental samples showed that addition of GFP–Tmod4 resulted in an increase in sarcomere structure (assayed by distinct M-line gaps) from 24% to 68%, compared with that of embryos treated with *lmod3* MO alone (Fig. 5Z). We observed that TFLs and sarcomere lengths for Tmod4-rescued Lmod3-depleted embryos were appreciably shorter than those of controls (*lmod3* MO+GFP–Tmod4: TFL, 0.74±0.04; sarcomere length, 1.99±0.08; versus control: TFL, 0.85±0.01; sarcomere length, 2.04±0.05; Table 1; mean±s.d.). The observed decrease in TFL was most likely due to the presence of excess GFP–Tmod4, given that overexpression of Tmod1 results in thin filament shortening (Sussman et al., 1999; Littlefield et al., 2001). These results indicate that Tmod4 is sufficient for the assembly of skeletal muscle myofibrils in embryos severely deficient in Lmod3.

The major difference between Tmod and Lmod proteins is the presence of a C-terminal extension with an additional actin-binding domain in Lmod proteins (Fig. 1A). We tested whether truncated versions of Lmod3, lacking the C-terminal extension, could incorporate into myofibrils and regulate skeletal muscle sarcomere assembly (supplementary material Fig. S4). Unlike full-length Lmod3 (supplementary material Fig. S3E–H), truncated versions of Lmod3 failed to assemble into the M-line region of sarcomeres in normal embryos (supplementary material Fig. S4A–H). Consistent with this observation, truncated versions of Lmod3 were unable to rescue myofibrillogenesis in embryos

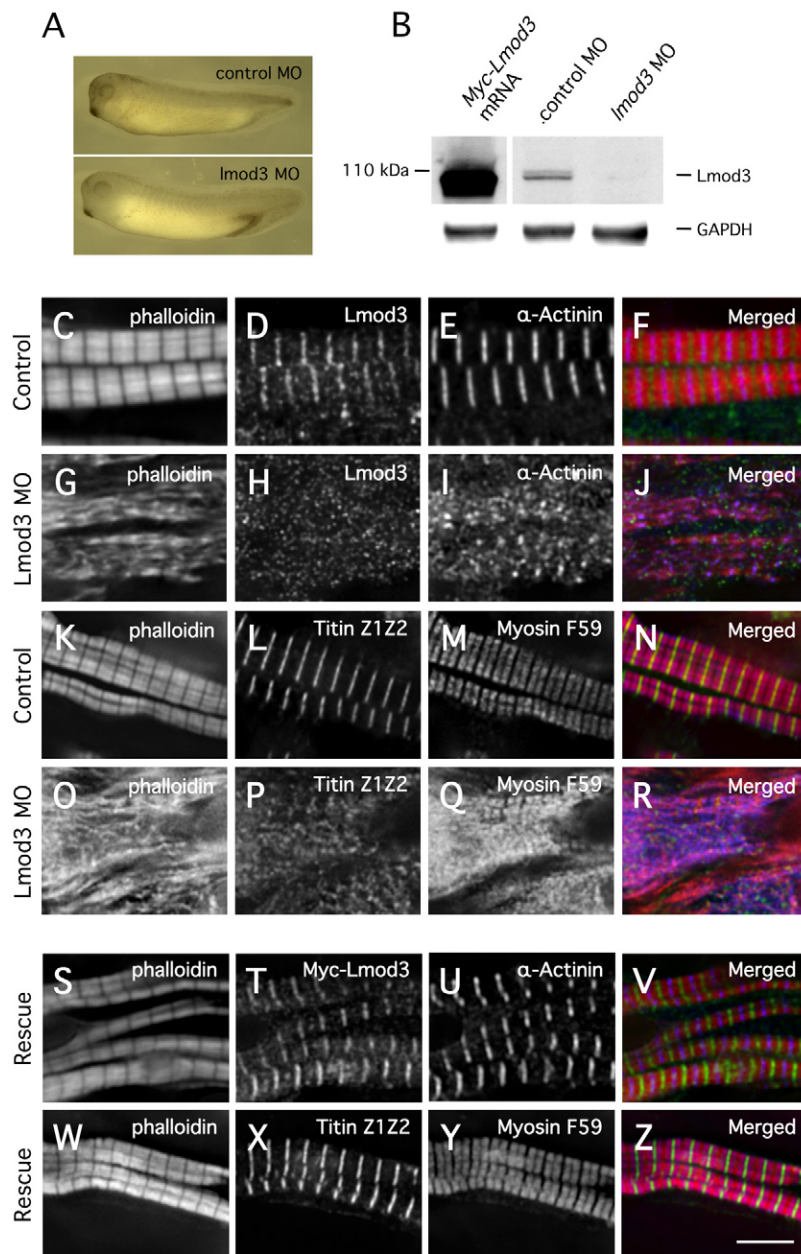
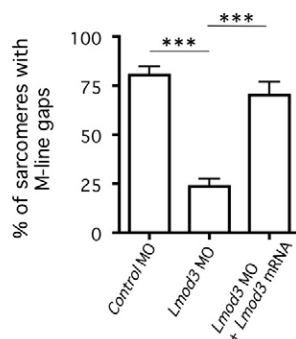


**Fig. 4. Lmod3 is essential for skeletal myofibril assembly.**

(A) Embryos treated with control MO (upper panel) and *lmod3* MO (lower panel) develop normally. (B) Protein blots demonstrate that the anti-Lmod antibody specifically recognizes *Xenopus* Lmod3 protein (lane labeled Myc-Lmod3) and that the *lmod3* MO effectively blocked translation of Lmod3 protein. (C–R) Loss of Lmod3 protein resulted in disruption of sarcomere assembly. (G–J) Sections through developing muscle tissue in embryos depleted of Lmod3 protein show severely disrupted sarcomere structure compared with that of control embryos of the same developmental stage (C–F). (O–R) The localization of other sarcomeric components, including titin (P) and myosin (Q) was also severely disorganized compared with that of controls (K–N). (S–Aa) The specificity of the Lmod3 knockdown was demonstrated by rescue experiments. *lmod3* MO was co-injected into the *Xenopus* embryo with mRNA encoding Myc-Lmod3. Organization of thin filament (S–V) and other sarcomeric proteins (X,Y) was comparable to that of unmanipulated controls (C–F). Scale bar: 5 μm. Quantification of results (Aa) showed that depletion of Lmod3 protein in st34 embryos resulted in a dramatic reduction in the percentage of correctly structured sarcomeres (70.2% in control MO-treated compared to 23.6% in *lmod3* MO-treated). The addition of mRNA encoding Myc-Lmod3 together with the *lmod3* MO restored sarcomere structure to control levels. Data show the mean ± s.e.m.; \*\*\* $P < 0.001$  ( $\chi^2$  analysis).

**Aa**



depleted of Tmod4 (supplementary material Fig. S4U–Zb). Western blots (supplementary material Fig. S4Ac) confirmed that the truncated versions of Lmod3 were expressed at

equivalent levels to the full-length Lmod3 protein that successfully rescued sarcomere structure (supplementary material Fig. S4Q–T).

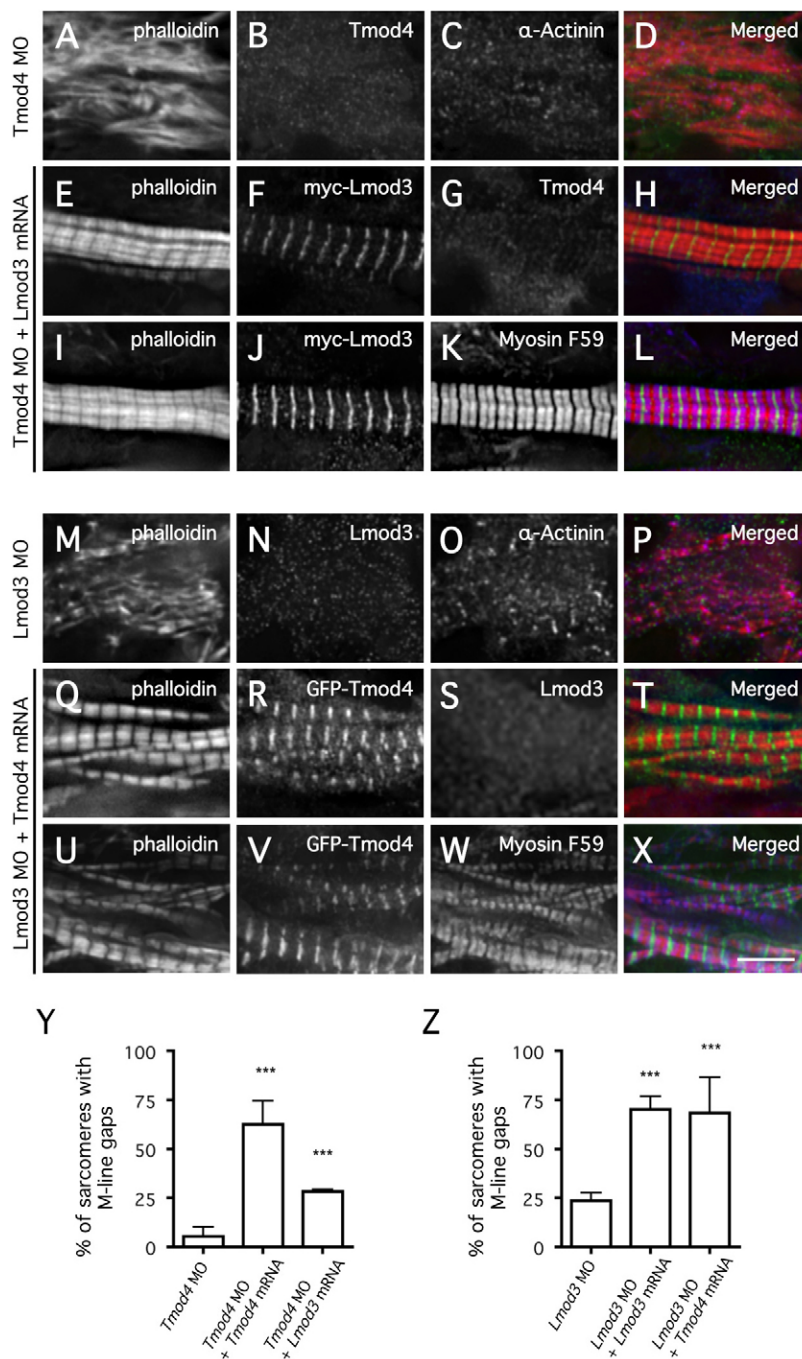


**Fig. 5. Lmod3 and Tmod4 display largely equivalent functions during skeletal myofibril assembly.** (A–L) In these studies, *tmod4* MO was co-injected into the *Xenopus* embryo along with mRNA encoding Myc–Lmod3. (E–L) When Myc–Lmod3 was added to embryos depleted of Tmod4, sarcomere assembly was significantly rescued compared with that of embryos depleted of Tmod4 alone (A–D). Note that in regions showing clear striated organization, Myc–Lmod3 was abundant at the M-line (F,J), whereas Tmod4 was not detected (G). The structure of other sarcomeric proteins, assayed by localization of myosin (K) was also restored. (M–X) In these studies, *lmod3* MO was co-injected into the *Xenopus* embryo along with mRNA encoding GFP–Tmod4 (Q–X). When GFP–Tmod4 was added to embryos depleted of Lmod3, sarcomere assembly was significantly rescued compared with that of embryos depleted of Lmod3 alone (M–P). Note that in regions showing mature striated organization, GFP–Tmod4 was abundant at the M-line (R,V), whereas Lmod3 was not detected (S). The structure of other sarcomeric proteins, assayed by the localization of myosin (W) was also restored. Scale bar: 5  $\mu$ m. (Y,Z) Quantification of experimental results showed that the addition of Myc–Lmod3 to embryos depleted of Tmod4 resulted in a significant increase in the percentage of sarcomeres displaying normal structure compared with that of Tmod4-depleted embryos (5.6-fold increase). Similarly, addition of GFP–Tmod4 to embryos depleted of Lmod3 resulted in a dramatic rescue of sarcomere structure compared with that observed in Lmod3-depleted muscle (2.9-fold). Data show the mean  $\pm$  s.e.m.; \*\*\* $P < 0.001$  ( $\chi^2$  analysis).

### Embryo locomotion is improved upon rescue of Tmod4 and Lmod3

To assess whether partial structural recovery at the subcellular level translated to improved physiological function, we conducted embryo locomotion (motility) assessments using a qualitative index-scoring matrix (Sadikot et al., 2010). Stage 34 embryos were scored on a scale of 0–5 for their response to an external stimulus (touching with forceps). This assay revealed that Tmod4-depleted embryos expressing mostly Lmod3, and Lmod3-depleted embryos expressing mostly Tmod4, displayed significantly improved locomotion compared with that of embryos treated with MO alone (Fig. 6). Owing to the complexity of controlling the levels and distribution of the rescuing protein in the live embryo, we predicted that rescue of

full locomotion would be difficult to achieve. However, statistically significant improvements in embryo locomotion were detected, indicating not only that Tmod4 and Lmod3 can compensate structurally for each other but that they appear to possess physiologically relevant redundant functions.

### DISCUSSION

#### Tmod4 and Lmod3 coexist at the M-line from early stages of myofibrillogenesis

We sought to explore the functions of the Tmod and Lmod family of actin filament regulatory proteins during *de novo* skeletal myofibrillogenesis. Our results indicate that *Xenopus* embryos are a powerful *in vivo* developmental model for the study of skeletal muscle assembly. Not only does the embryo form functional



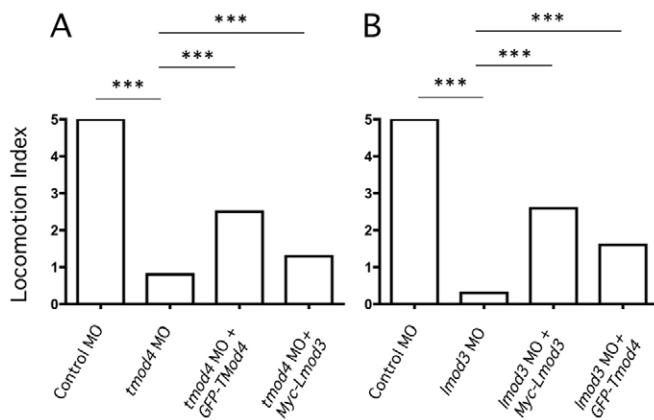


**Fig. 6. Locomotion assays for embryonic muscle function.** Embryos were assayed at st34 for locomotion using a qualitative index scale of 0–5 (Sadikot et al., 2010). (A) Embryos depleted of Tmod4 showed very little motility compared with control embryos. However, addition of either GFP–Tmod4 (homologous rescue) or Myc–Lmod3 (heterologous rescue) resulted in a significant increase in embryo motility. (B) Embryos depleted of Lmod3 showed very little movement compared with control embryos. However, addition of either Myc–Lmod3 protein (homologous rescue) or GFP–Tmod4 protein (heterologous rescue) resulted in a significant increase in embryo motility. Data show the means; \*\*\* $P < 0.001$  ( $\chi^2$  analysis). Embryo numbers assayed are as follows: control, 40; *lmod3* MO, 30; *tmod4* MO, 35; *lmod3* MO+Myc–Lmod3, 12; *tmod4* MO+GFP–Tmod4, 24; *lmod3* MO+GFP–Tmod4, 13; and *tmod4* MO+Myc–Lmod3, 32.

skeletal muscle in <3 days, but also it is extremely compliant to protein level manipulations during its development. This facilitates elucidation of the crucial protein components and regulatory pathways involved in building a myofibril *in vivo*. We found for the first time that Tmod4 and Lmod3 share similar structural and functional roles during initial assembly of the embryonic sarcomere. This result was unexpected based on the significant differences in domain structure of the two proteins, including the presence of a second tropomyosin-binding domain in Tmods and the presence of a WH2-containing C-terminal extension in Lmods. In addition, *in vitro* and cell culture studies of other Lmod and Tmod family members have demonstrated different localizations, assembly patterns and functional properties of the molecules (e.g. Lmod2 is a robust actin filament nucleator and an elongation factor, whereas Tmod1 functions as a capping protein).

Expression of all Tmod and Lmod genes was analyzed in the developing *Xenopus* embryo. These experiments showed that only Tmod4 and Lmod3 were expressed at high levels in skeletal muscle (Fig. 1), suggesting that these isoforms are the most relevant during myofibril assembly. The observation that Tmod4 and Lmod3 are coexpressed during early skeletal myofibrillogenesis is different from that observed in cardiac myocytes, where Tmod1 expression substantially precedes Lmod2 expression (Tsukada et al., 2010; Skwarek-Maruszewska et al., 2010).

During *Xenopus* development, sarcomere structure is first detected in developing skeletal muscle tissue of the st24 somites (Muntz 1975). Consistent with these previous studies, we were unable to detect sarcomere structure in st20 embryos (Fig. 2A–D,M–P), but thin and immature myofibrils were detected ~5 hours later in st24 embryos (Huang and Hockaday, 1988). Prior to sarcomere assembly, Tmod4 and Lmod3 were distributed in a punctate pattern (Fig. 2). This observation is consistent with a previous study showing that Tmod4 (sk-Tmod) associated with

developing nonstriated immature myofibrils in cultured chick skeletal myotubes (Almenar-Queralt et al., 1999a). At later developmental stages, mature myofibrils were present throughout the skeletal muscle of the trunk of the embryo, and both Tmod4 and Lmod3 localization persisted in the M-line region. Until this study, the localization of Lmod3 during embryonic striated muscle development was unknown. These localization studies suggest that both proteins have roles during the assembly and maintenance of myofibrils.

Prior studies have reported that Lmod2 and Tmod1 localize differently within myofibrils in cultured chick cardiac myocytes. Specifically, Lmod2 was only found to be associated with mature myofibrils as two broader bands, which appeared to be more separated from M-lines than Tmod1 (Skwarek-Maruszewska et al., 2010). We did not observe differential localization patterns or differences in the timing of assembly for Lmod3 and Tmod4. At the expression levels used in our studies, epitope-tagged Tmod4 protein did not appear to displace endogenous Lmod3, nor did tagged Lmod3 displace Tmod4 (supplementary material Fig. S3A–H). This was unexpected based on experiments in chick primary cardiac myocytes, where high-level expression of Lmod2 resulted in the displacement of Tmod1 from thin filament pointed ends (Tsukada et al., 2010). Although our observations suggest that Tmod4 and Lmod3 localize simultaneously at the actin thin filament pointed ends, it is still not clear whether they localize to the same or different thin filaments. According to a model proposed by Kostyukova and colleagues, Tmod caps thin filament ends by interacting with two tropomyosin molecules through its two tropomyosin binding sites (Kostyukova et al., 2006). To date, no reports have been published on the association of Lmod with actin filament pointed ends, although it has been reported that Lmod–tropomyosin and Tmod–tropomyosin interactions are isoform specific (Kostyukova et al., 2006; Kostyukova, 2007; Kostyukova, 2008). During early skeletal muscle development in *Xenopus*, several isoforms of tropomyosin are expressed, including the  $\alpha 2$ ,  $\alpha 7$ ,  $\beta 4$  and  $\beta 5$  isoforms (Hardy and Thiébaud, 1992; Hardy et al., 1999). Hence, it is possible that the tropomyosin composition of the thin filaments could influence preferential association of Tmods or Lmods with specific thin filament pointed ends.

When additional GFP–Tmod4 or Myc–Lmod3 was overexpressed in otherwise normal embryos, no alterations in TFL were observed (supplementary material Fig. S3A–H; Table 1). This suggests either that Tmod4 and Lmod3 do not have roles in length specification during early skeletal myofibril assembly or that the levels of additional tagged Lmod and Tmod proteins expressed were not sufficient to promote changes in TFL *in vivo*.

### Tmod4 is essential for skeletal muscle development and locomotion

Relatively little is known concerning the precise roles of Tmod4 and Lmod3 during skeletal muscle development. To address this question, we used specific translation-blocking MOs to inhibit synthesis of the respective proteins. Protein blots indicated that the *tmod4* MO was very effective in reducing Tmod4 protein levels in treated embryos relative to those of controls (Fig. 3B). It is intriguing that the result of Tmod4 depletion is much more global than simply altering TFLs. Knockdown of Tmod4 resulted in major defects in myofibrillogenesis with severely compromised sarcomere formation. The effect of Tmod4 knockdown that we observed in skeletal muscle is consistent with the previously reported disruption of sarcomere structure in the hearts of Tmod1-

null E9.5 embryos and in Tmod1-null cardiomyocytes derived from murine embryonic stem cells (Fritz-Six et al., 2003; Chu et al., 2003; Ono et al., 2005).

In some developing muscle regions of the embryo, partial sarcomere structure could be recognized, but in the majority of regions, sarcomere structure was absent. We are unable to determine whether the partial structure was due to incomplete knockdown of Tmod4 protein or whether some sarcomere assembly is possible in the absence of Tmod4 protein. Compensation by other Tmod family members is unlikely for two reasons. First, no detectable alteration in expression levels of Tmod and Lmod family genes was observed in response to MO treatment (supplementary material Fig. S2). Second, immunofluorescent staining and western blots using polyclonal antibodies that recognize all isoforms (Fig. 3B; Fig. 4B), showed very low levels of total Tmod and Lmod protein at the time of assay.

Most importantly, expression of GFP–Tmod4 in *tmod4* MO-treated embryos restored thin filament organization and myofibril assembly (Fig. 3) and, partially, the ability of the embryo to swim (Fig. 6), demonstrating the specificity of the loss-of-function phenotype. Our results show, for the first time, that Tmod4 is crucial for successful sarcomere assembly in embryonic skeletal muscle.

### **Lmod3 is essential for skeletal muscle development and tadpole motility**

We carried out equivalent studies to determine whether Lmod3 has an essential function during skeletal myofibrillogenesis. Again, Lmod3 knockdown affected the overall formation of sarcomeres, not simply TFL. Embryos treated with *lmod3* MO showed regions of severe myofibril disorganization throughout the developing musculature. These results are similar to the Lmod2 knockdown studies in cultured cardiomyocytes (Chereau et al., 2008). Interestingly, reduced Lmod3 levels also severely compromised the locomotion of the tadpole (Fig. 6). Homologous-rescue experiments effectively restored myofibril organization, thin filament structure and organization compared with those of *lmod3* MO-treated embryos (Table 1). The addition of *lmod3* mRNA to the *lmod3* MO-treated embryos also significantly rescued their swimming activity (Fig. 6). These studies demonstrate, for the first time, that the function of an Lmod family member is essential for skeletal muscle myofibrillogenesis.

### **Alternate rescue experiments reveal functional redundancies between Lmod3 and Tmod4**

Because Tmod and Lmod possess different biochemical properties (e.g. Tmod1 acts as a capping protein and Lmod2 acts as a nucleator and an elongation factor) it was surprising to observe that the addition of excess Lmod3 was able to partially rescue the *tmod4* MO-treated embryos and vice versa. These studies raise the question of the respective functions of Lmod3 and Tmod4 during sarcomere assembly. We can propose two broadly different models. In the first, Lmod3 and Tmod4 proteins play unique roles during sarcomere formation. For example, a defined ratio of the two proteins with no overlapping functions might be required to regulate TFL within parameters consistent with myofibrillogenesis. In the second model, Lmod3 and Tmod4 might perform broadly similar functions during myofibrillogenesis. In this case, the most important factor might be the appropriate levels of total (Lmod plus Tmod) protein. This second model is consistent with the observation that Tmods and Lmods are members of a larger family that share many of the same functional domains [approximately two

thirds of the Lmod sequence resembles that of Tmod (Fig. 1A; Conley et al., 2001)].

Studies of cardiac myocytes in culture indicated that a truncated version of Lmod2 protein, lacking the C-terminal extension, could incorporate into myofibrils and shorten actin filaments (Tsukada et al., 2010). However, we were unable to observe any incorporation of truncated versions of Lmod3 proteins into sarcomeres, either in the context of normal sarcomere assembly (supplementary material Fig. S4A–H), or in embryos depleted of Tmod4 (supplementary material Fig. S4U–Ab). A number of reasons might be considered for the difference in observed results, including the different Lmod isoforms examined, structural differences between skeletal muscle and cardiac muscle, levels of endogenous Lmod protein competing for assembly into the myofibril and/or expression levels of the truncated protein. Given that significant levels of endogenous Lmod3 are present at the time of sarcomere assembly in *Xenopus* (Fig. 2), the most likely explanation is that the truncated version of Lmod3 is unable to successfully compete with the endogenous full-length protein at the levels of overexpression used in these studies.

In order to interpret our results, it might be useful to consider the relative amounts of Lmod3 and Tmod4 proteins during normal myofibrillogenesis and during the different experimental manipulations. As we showed using fluorescent microscopy (Fig. 2), both Lmod3 and Tmod4 proteins were detected at the M-line region as early as any sarcomere structures were present. Although we do not know the stoichiometry of the two proteins at this time, they are clearly present at a concentration that facilitates myofibril formation. When Tmod4 protein is specifically reduced, Lmod3 protein remains present at normal levels (data not shown). However, these levels are not compatible with efficient sarcomere formation, either because Tmod4 has a unique function or because the total amount of Lmod3 plus Tmod4 is no longer sufficient. An equivalent situation applies when Lmod3 protein levels are reduced and sarcomere structure is severely disrupted. Either Lmod3 is required for a unique function, or the total amount of Lmod3 plus Tmod4 is inadequate for efficient sarcomere formation.

We believe that the results of homologous versus heterologous rescue studies allow us to distinguish between the two models presented above. When Tmod4 was specifically reduced, Lmod3 levels were unchanged, but sarcomere assembly was severely disrupted. However, addition of Myc–Lmod3 was sufficient to rescue sarcomere assembly and structure. In this situation, Lmod3 effectively provided the crucial total of Lmod3 plus Tmod4. Similarly, Lmod3 depletion could be rescued by increasing the levels of Tmod4, in the form of additional GFP–Tmod4. Although previous studies have shown that Lmod and Tmod possess distinct properties and work in competition to fine tune the length of thin filaments, our studies extend this model by suggesting that efficient sarcomere formation can occur provided that sufficient amounts of either protein are present. In this case, the similarities in protein structure between the Lmod and Tmod families are more important than the differences. This interpretation is consistent with studies of myofibril formation in cardiac muscle. Previous studies have shown that transcripts for Lmod2 are not present in developing chick cardiac tissue until after myofibrillogenesis has occurred and the heart is beating (Tsukada et al., 2010). This observation strongly implies that the presence of Tmod1 alone is sufficient for myofibril assembly in the heart. The addition of Lmod2 protein during later stages of

cardiogenesis is consistent with the observed lengthening of cardiac thin filaments as development proceeds (Tsukada et al., 2010).

Our studies also make a link between myofibril organization and functional activity at the physiological level. In both heterologous rescue experiments, the locomotion of the tadpoles was partially restored. Although there can be many interpretations, we predict that an increased presence of regulated thin filaments maintains sufficient acto-myosin interactions to allow efficient swimming.

## MATERIALS AND METHODS

### Leiomodlin 1–3 and tropomodulin 1–4 constructions

The following plasmids containing *Xenopus* Lmod1–3 and Tmod1–4 sequences were obtained from Thermo Scientific (Thermo Scientific, Pittsburgh, PA): Tmod1, 6874337; Tmod2, 7606904; Tmod3, 7689916; Tmod4, 3396511; Lmod1, 7866366; Lmod2, 7733245; Lmod3, 7850238. The orthology of genes was confirmed using Xenbase (Bowes et al., 2008). Plasmids were linearized and used as a template to generate RNA probes suitable for *in situ* hybridization analysis (Harland, 1991). For mRNA synthesis, full-length or truncated coding regions of Lmod3 (NM\_001079212) and Tmod4 (NM\_001016737) were amplified using PCR and inserted into pT7TS vectors containing an N-terminal Myc or GFP tag. Full-length mRNAs encoding Myc–Lmod3 and GFP–Tmod4 were prepared using the T7 mMACHINE kit (Ambion/Life Technologies Carlsbad, CA).

### Microinjections

Morpholinos (MOs) and mRNAs were microinjected into one-cell-stage *Xenopus* embryos incubated in 0.2× MMR/6% Ficoll. Embryos were allowed to recover in 0.2× MMR/2% Ficoll, transferred to 0.2× MMR and processed at st34 (tailbud stage). For knockdown studies, we used Lmod3 and Tmod4 translation-blocking antisense MOs (*lmod3* MO1, 5'-CTTGGTCCGAACCCTGGGACATTAT-3'; *lmod3* MO2, 5'-AGGTTT-TTATTGGCAGGTTCCGCA-3'; *tmod4* MO, 5'-AGCTCCTTCTG-GTAAGACATGTTGG-3'; Gene Tools, LLC, Philomath, OR). MOs were injected at 37.5 ng for *tmod4* and 25 ng each of *lmod3* MO1 and MO2 (total 50 ng). For MO control experiments, we used a mismatch *myh6* MO (5'-TCTCCGATCATCGCATGAGCCATTG-3') at 50 ng. For protein localization studies, 300 pg of mRNA encoding Myc–Lmod3 and GFP–Tmod4 was injected. For Lmod3 and Tmod4 rescue studies, 900 pg of Myc–Lmod3 or GFP–Tmod4 mRNA was injected, together with the MO doses described above.

### Western blot analysis

*Xenopus* lysate preparation was adapted from a method described previously (Vaughan et al., 2011). Briefly, total protein from 20 embryos was separated using pre-cast 10% polyacrylamide gels (Bio-Rad, Hercules, CA). Bicinchoninic acid assays and Ponceau S stains verified equivalent protein loading. Western blots were performed as described previously (Bliss et al., 2013) using rabbit anti-Tmod (1:1000), rabbit anti-Lmod3 (1:1000; Proteintech, Chicago, IL), monoclonal anti-GFP (1:3000; Covance, Dedham, MA), monoclonal anti-GAPDH (1:30,000; Sigma, St Louis, MO) and monoclonal anti-Myc (1:1000, Upstate Biotechnology/Millipore, Billerica, MA; clone 9E10) antibodies.

### Immunofluorescence microscopy

Embryos were prepared for cryosectioning and immunofluorescent staining as described previously (Nworu et al., 2013). The primary antibodies included a monoclonal anti- $\alpha$ -actinin (1:10,000; Sigma-Aldrich), rabbit anti-GFP (1:300; Abcam, Cambridge, UK), monoclonal anti-GFP (1:300; Invitrogen, Carlsbad, CA), rabbit anti-Myc (1:300; Upstate Biotechnology/Millipore), monoclonal anti-Myc (1:300; Upstate Biotechnology/Millipore; clone 9E10), rabbit anti-Tmod (1:500) and a rabbit anti-Lmod3 antibody (1:300; Proteintech). Texas-Red-conjugated phalloidin (1:400; Invitrogen) was used to stain F-actin. The secondary

antibodies obtained from Invitrogen and Jackson ImmunoResearch Laboratories, Inc. included Alexa-Fluor-488-conjugated goat anti-mouse-IgG (1:500), Alexa-Fluor-488-conjugated goat anti-rabbit-IgG (1:500), Cy5-conjugated goat anti-mouse-IgG (1:500) and Cy5-conjugated donkey anti-rabbit-IgG (1:500). Coverslips were mounted onto slides with Aqua Poly/Mount (Polysciences, Inc., Warrington, PA). The sections were imaged using a Deltavision RT system (Applied Precision, Issaquah, WA) with an inverted microscope (IX70; Olympus), a 100× NA 1.3 objective and a CoolSNAP HQ digital camera (Photometrics, Tucson, AZ) using SoftWoRx 3.5.1 software (Applied Precision). The images were deconvolved with SoftWoRx and then processed using Photoshop CS (Adobe, San Jose, CA).

### Structural analysis and length measurements

For all structural studies, three image sets of Texas-Red–phalloidin- and anti- $\alpha$ -actinin-stained sections were acquired from three or four embryos per treatment. Only somite regions showing GFP fluorescence were analyzed. Images of sarcomeric  $\alpha$ -actinin and phalloidin staining were merged;  $\alpha$ -actinin was used to identify sarcomeres and sarcomere lengths and phalloidin was used to measure TFLs. Gaps in phalloidin staining at the M-line were recorded. Chi square analysis was used to determine statistical significance. Results of four independent experiments were analyzed. TFLs and sarcomere lengths were quantified using the DDecon plugin for ImageJ 1.42q software; this software was generously provided by Dr David Gokhin and Dr Velia Fowler (The Scripps Research Institute, La Jolla, CA) (Littlefield and Fowler, 2002; Gokhin et al., 2010). A Student's *t*-test was performed to test for significance. Locomotion analysis was performed as described previously (Sadikot et al., 2010). Briefly, st34 control and experimental embryos were scored on a scale of 0–5 for their ability to twitch or swim in response to an external stimulus.

### Acknowledgements

We thank members of the Gregorio and Krieg laboratories for thoughtful discussions. We thank Cathleen Cover and Christine Henderson for help with western blots, David Gokhin and Velia Fowler for their Distributed Deconvolution (DDecon) software and Rachel Bennett for DDecon length measurements.

### Competing interests

The authors declare no competing or financial interests.

### Author contributions

C.U.N. carried out the majority of the experiments. D.C.S. and R.K. performed the *in situ* hybridization analysis and the Lmod3 truncation studies, respectively. C.U.N., P.A.K. and C.C.G. conceived, planned and evaluated the experiments. C.U.N., C.C.G. and P.A.K. wrote the manuscript. C.C.G. and P.A.K. contributed equally to this work.

### Funding

This work was supported by funding from the Steven M. Gootter Foundation; and the National Institutes of Health (NIH) [grant number HL093694] to P.A.K., funding from NIH [grant numbers HL108625 and HL083146] to C.C.G.; and More Graduate Education at Mountain States Alliance; and Western Alliance to Expand Student Opportunities to C.U.N. Deposited in PMC release after 12 months.

### Supplementary material

Supplementary material available online at <http://jcs.biologists.org/lookup/suppl/doi:10.1242/jcs.152702/-DC1>

### References

- Almenar-Queral, A., Gregorio, C. C. and Fowler, V. M. (1999a). Tropomodulin assembles early in myofibrillogenesis in chick skeletal muscle: evidence that thin filaments rearrange to form striated myofibrils. *J. Cell Sci.* **112**, 1111–1123.
- Almenar-Queral, A., Lee, A., Conley, C. A., Ribas de Pouplana, L. and Fowler, V. M. (1999b). Identification of a novel tropomodulin isoform, skeletal tropomodulin, that caps actin filament pointed ends in fast skeletal muscle. *J. Biol. Chem.* **274**, 28466–28475.
- Bang, M. L., Li, X., Littlefield, R., Bremner, S., Thor, A., Knowlton, K. U., Lieber, R. L. and Chen, J. (2006). Nebulin-deficient mice exhibit shorter thin filament lengths and reduced contractile function in skeletal muscle. *J. Cell Biol.* **173**, 905–916.

- Bliss, K. T., Chu, M., Jones-Weinert, C. M. and Gregorio, C. C. (2013). Investigating lasp-2 in cell adhesion: new binding partners and roles in motility. *Mol. Biol. Cell* **24**, 995–1006.
- Bowes, J. B., Snyder, K. A., Segerdell, E., Gibb, R., Jarabek, C., Noumen, E., Pollet, N. and Vize, P. D. (2008). Xenbase: a *Xenopus* biology and genomics resource. *Nucleic Acids Res.* **36**, D761–D767.
- Chereau, D., Boczkowska, M., Skwarek-Maruszewska, A., Fujiwara, I., Hayes, D. B., Rebowski, G., Lappalainen, P., Pollard, T. D. and Dominguez, R. (2008). Leiomodins are actin filament nucleators in muscle cells. *Science* **320**, 239–243.
- Chu, X., Chen, J., Reedy, M. C., Vera, C., Sung, K. L. P. and Sung, L. A. (2003). E-Tmod capping of actin filaments at the slow-growing end is required to establish mouse embryonic circulation. *Am. J. Physiol.* **284**, 1827–1838.
- Conley, C. A., Fritz-Six, K. L., Almenar-Queralt, A. and Fowler, V. M. (2001). Leiomodins: larger members of the tropomodulin (Tmod) gene family. *Genomics* **73**, 127–139.
- Fowler, V. M., Greenfield, N. J. and Moyer, J. (2003). Tropomodulin contains two actin filament pointed end-capping domains. *J. Biol. Chem.* **278**, 40000–40009.
- Fritz-Six, K. L., Cox, P. R., Fischer, R. S., Xu, B., Gregorio, C. C., Zoghbi, H. Y. and Fowler, V. M. (2003). Aberrant myofibril assembly in tropomodulin1 null mice leads to aborted heart development and embryonic lethality. *J. Cell Biol.* **163**, 1033–1044.
- Gokhin, D. S. and Fowler, V. M. (2011). Cytoplasmic  $\gamma$ -actin and tropomodulin isoforms link to the sarcoplasmic reticulum in skeletal muscle fibers. *J. Cell Biol.* **194**, 105–120.
- Gokhin, D. S., Bang, M. L., Zhang, J., Chen, J. and Lieber, R. L. (2009). Reduced thin filament length in nebulin-knockout skeletal muscle alters isometric contractile properties. *Am. J. Physiol.* **296**, 1123–1132.
- Gokhin, D. S., Lewis, R. A., McKeown, C. R., Nowak, R. B., Kim, N. E., Littlefield, R. S., Lieber, R. L. and Fowler, V. M. (2010). Tropomodulin isoforms regulate thin filament pointed-end capping and skeletal muscle physiology. *J. Cell Biol.* **189**, 95–109.
- Granzier, H., Akster, H. A. and Ter Keurs, H. (1991). Effect of thin filament length on the force-sarcomere length relation of skeletal muscle. *Am. J. Physiol.* **260**, 1060–1070.
- Greenfield, N. J., Kostyukova, A. S. and Hitchcock-DeGregori, S. E. (2005). Structure and tropomyosin binding properties of the N-terminal capping domain of tropomodulin 1. *Biophys. J.* **88**, 372–383.
- Gregorio, C. C., Weber, A., Bondad, M., Pennise, C. R. and Fowler, V. M. (1995). Requirement of pointed-end capping by tropomodulin to maintain actin filament length in embryonic chick cardiac myocytes. *Nature* **377**, 83–86.
- Hardy, S. and Thiébaud, P. (1992). Isolation and characterization of cDNA clones encoding the skeletal and smooth muscle *Xenopus laevis* beta tropomyosin isoforms. *Biochim. Biophys.* **1131**, 239–242.
- Hardy, S., Hamon, S., Cooper, B., Mohun, T. and Thiébaud, P. (1999). Two skeletal  $\alpha$ -tropomyosin transcripts with distinct 3'UTR have different temporal and spatial patterns of expression in the striated muscle lineages of *Xenopus laevis*. *Mech. Dev.* **87**, 199–202.
- Harland, R. M. (1991). In situ hybridization: an improved whole-mount method for *Xenopus* embryos. *Methods Cell Biol.* **36**, 685–695.
- Holtzer, H., Hijikata, T., Lin, Z. X., Zhang, Z. Q., Holtzer, S., Protasi, F., Franzini-Armstrong, C. and Sweeney, H. L. (1997). Independent assembly of 1.6 microns long bipolar MHC filaments and I-Z-I bodies. *Cell Struct Funct.* **22**, 83–93.
- Huang, C. L. and Hockaday, A. R. (1988). Development of myotomal cells in *Xenopus laevis* larvae. *J. Anat.* **159**, 129–136.
- Kong, K. Y. and Kedes, L. (2006). Leucine 135 of tropomodulin-1 regulates its association with tropomyosin, its cellular localization, and the integrity of sarcomeres. *J. Biol. Chem.* **281**, 9589–9599.
- Kostyukova, A. S. (2007). Leiomodins/tropomyosin interactions are isoform specific. *Arch. Biochem. Biophys.* **465**, 227–230.
- Kostyukova, A. S. (2008). Tropomodulins and tropomodulin/tropomyosin interactions. *Cell. Mol. Life Sci.* **65**, 563–569.
- Kostyukova, A. S., Rapp, B. A., Choy, A., Greenfield, N. J. and Hitchcock-DeGregori, S. E. (2005). Structural requirements of tropomodulin for tropomyosin binding and actin filament capping. *Biochemistry* **44**, 4905–4910.
- Kostyukova, A. S., Choy, A. and Rapp, B. A. (2006). Tropomodulin binds two tropomyosins: a novel model for actin filament capping. *Biochemistry* **45**, 12068–12075.
- Littlefield, R., Almenar-Queralt, A. and Fowler, V. M. (2001). Actin dynamics at pointed ends regulates thin filament length in striated muscle. *Nat. Cell Biol.* **3**, 544–551.
- Littlefield, R. and Fowler, V. M. (2002). Measurement of thin filament lengths by distributed deconvolution analysis of fluorescence images. *Biophys. J.* **82**, 2548–2564.
- McKeown, C. R., Nowak, R. B., Moyer, J., Sussman, M. A. and Fowler, V. M. (2008). Tropomodulin1 is required in the heart but not the yolk sac for mouse embryonic development. *Circ. Res.* **103**, 1241–1248.
- Mohun, T. J., Brennan, S., Dathan, N., Fairman, S. and Gurdon, J. B. (1984). Cell type-specific activation of actin genes in the early amphibian embryo. *Nature* **311**, 716–721.
- Mudry, R. E., Perry, C. N., Richards, M., Fowler, V. M. and Gregorio, C. C. (2003). The interaction of tropomodulin with tropomyosin stabilizes thin filaments in cardiac myocytes. *J. Cell Biol.* **162**, 1057–1068.
- Muntz, L. (1975). Myogenesis in the trunk and leg during development of the tadpole of *Xenopus laevis* (Daudin 1802). *J. Embryol. Exp. Morphol.* **33**, 757–774.
- Nanda, V. and Miano, J. M. (2012). Leiomodins 1, a new serum response factor-dependent target gene expressed preferentially in differentiated smooth muscle cells. *J. Biol. Chem.* **287**, 2459–2467.
- Nworu, C. U., Krieg, P. A. and Gregorio, C. C. (2013). Preparation of developing *Xenopus* muscle for sarcomeric protein localization by high-resolution imaging. *Methods* **66**, 370–379.
- Ono, S. (2010). Dynamic regulation of sarcomeric actin filaments in striated muscle. *Cytoskeleton* **67**, 677–692.
- Ono, Y., Schwach, C., Antin, P. B. and Gregorio, C. C. (2005). Disruption in the tropomodulin1 (Tmod1) gene compromises cardiomyocyte development in murine embryonic stem cells by arresting myofibril maturation. *Dev. Biol.* **282**, 336–348.
- Ottenheijm, C. A., Witt, C. C., Stienen, G. J., Labeit, S., Beggs, A. H. and Granzier, H. (2009). Thin filament length dysregulation contributes to muscle weakness in nemaline myopathy patients with nebulin deficiency. *Hum. Mol. Genet.* **18**, 2359–2369.
- Rhee, D., Sanger, J. M. and Sanger, J. W. (1994). The premyofibril: evidence for its role in myofibrillogenesis. *Cell Motil. Cytoskeleton* **28**, 1–24.
- Sadikot, T., Hammond, C. R. and Ferrari, M. B. (2010). Distinct roles for telethonin N-versus C-terminus in sarcomere assembly and maintenance. *Dev. Dyn.* **239**, 1124–1135.
- Skwarek-Maruszewska, A., Boczkowska, M., Zajac, A. L., Kremneva, E., Svitkina, T., Dominguez, R. and Lappalainen, P. (2010). Different localizations and cellular behaviors of leiomodins and tropomodulin in mature cardiomyocyte sarcomeres. *Mol. Biol. Cell* **21**, 3352–3361.
- Sparrow, J. C. and Schöck, F. (2009). The initial steps of myofibril assembly: integrins pave the way. *Nat. Rev. Mol. Cell Biol.* **10**, 293–298.
- Sussman, M. A., Baqué, S., Uhm, C. S., Daniels, M. P., Price, R. L., Simpson, D., Terracio, L. and Kedes, L. (1998). Altered expression of tropomodulin in cardiomyocytes disrupts the sarcomeric structure of myofibrils. *Circ. Res.* **82**, 94–105.
- Sussman, M. A., Welch, S., Gude, N., Khoury, P. R., Daniels, S. R., Kirkpatrick, D., Walsh, R. A., Price, R. L., Lim, H. W. and Molkenin, J. D. (1999). Pathogenesis of dilated cardiomyopathy: molecular, structural, and population analyses in tropomodulin-overexpressing transgenic mice. *Am. J. Pathol.* **155**, 2101–2113.
- Tsukada, T., Pappas, C. T., Moroz, N., Antin, P. B., Kostyukova, A. S. and Gregorio, C. C. (2010). Leiomodins 2 is an antagonist of tropomodulin-1 at the pointed end of the thin filaments in cardiac muscle. *J. Cell Sci.* **123**, 3136–3145.
- Tsukada, T., Kotlyanskaya, L., Huynh, R., Desai, B., Novak, S. M., Kajava, A. V., Gregorio, C. C. and Kostyukova, A. S. (2011). Identification of residues within tropomodulin-1 responsible for its localization at the pointed ends of the actin filaments in cardiac myocytes. *J. Biol. Chem.* **286**, 2194–2204.
- Vaughan, E. M., Miller, A. L., Yu, H. Y. and Bement, W. M. (2001). Control of local Rho GTPase crosstalk by Abr. *Curr Biol.* **21**, 270–277.
- Watakabe, A., Kobayashi, R. and Helfman, D. M. (1996). N-tropomodulin: a novel isoform of tropomodulin identified as the major binding protein to brain tropomyosin. *J. Cell Sci.* **109**, 2299–2310.
- Weber, A., Pennise, C. R., Babcock, G. G. and Fowler, V. M. (1994). Tropomodulin caps the pointed ends of actin filaments. *J. Cell Biol.* **127**, 1627–1635.
- Witt, C. C., Burkart, C., Labeit, D., McNabb, M., Wu, Y., Granzier, H. and Labeit, S. (2006). Nebulin regulates thin filament length, contractility, and Z-disk structure in vivo. *EMBO J.* **25**, 3843–3855.
- Yamashiro, S., Gokhin, D. S., Kimura, S., Nowak, R. B. and Fowler, V. M. (2012). Tropomodulins: pointed-end capping proteins that regulate actin filament architecture in diverse cell types. *Cytoskeleton* **69**, 337–370.